

Elastic and anelastic behavior associated with magnetic ordering in the skyrmion host Cu_2OSeO_3 Kanta Adachi ^{*}*Department of Earth Sciences, University of Cambridge, Downing Street, Cambridge CB2 3EQ, United Kingdom
and Department of Systems Innovation Engineering, Iwate University, Morioka, Iwate 020-8551, Japan*Heribert Wilhelm *Helmholtz-Institute Ulm, Helmholtz-Straße 11, 89081 Ulm, Germany*

Marcus P. Schmidt

Max Planck Institute for Chemical Physics of Solids, 01187 Dresden, Germany

Michael A. Carpenter

Department of Earth Sciences, University of Cambridge, Downing Street, Cambridge CB2 3EQ, United Kingdom

(Received 24 October 2023; revised 2 February 2024; accepted 25 March 2024; published 17 April 2024)

Magnetic ordering in Cu_2OSeO_3 occurs without any detectable changes in the lattice symmetry but involves significant coupling with strain. The strain coupling effects in Cu_2OSeO_3 have been investigated with a focus on the skyrmion lattice by examining elastic and anelastic properties. Resonant ultrasound spectroscopy has been used to measure these properties of a Cu_2OSeO_3 single crystal as a function of temperature and magnetic field. On heating, the skyrmion phase has been characterized by slightly softer elasticity compared to the helical phase. However, there were no obvious anomalies in elastic and anelastic properties associated with the boundary of the stability field of the skyrmion lattice. Evolution of elastic properties with magnetic field, passing through the stability field of the skyrmion lattice, showed a characteristic pattern of a glassy state, where an equilibrium state is never reached. These imply that coupling of the skyrmions with strain is extremely weak in Cu_2OSeO_3 , leading to glassy or liquidlike behavior of skyrmions. Three Debye-like loss peaks were observed near ~ 40 , ~ 50 , and ~ 60 K. The relaxation mechanism for the 40 K loss peak has been found to have a single relaxation time. Overlapping acoustic loss peaks in the temperature interval ~ 50 – 62 K suggest that the magnetic transitions with variable temperature in this temperature range involve freezing of some dynamic aspect(s) of the magnetic structure with an activation energy of ~ 0.1 – 0.15 eV.

DOI: [10.1103/PhysRevB.109.144413](https://doi.org/10.1103/PhysRevB.109.144413)**I. INTRODUCTION**

Strain coupling is an important aspect of materials which undergo phase transitions. It is well understood that phase transitions are almost invariably accompanied by macroscopic distortions as a consequence of cooperative local changes such as magnetic ordering. Strain has a fundamental influence on not only an acoustic mode instability as the primary order parameter but also a wide variety of instabilities through coupling with other order parameters [1–3]. The coupling between strain and order parameter increases the correlation length of the order parameter because of the long-range nature of strain fields, promoting mean-field behavior of related thermodynamic properties. In addition, strain fields provide

a mechanism for indirect coupling between separate order parameters through common strains. Such mechanisms can result in strong coupling between different instabilities when strains that occur with one order parameter sufficiently overlap with strains coupled with another order parameter. In the context of domain-wall engineering [4–6], strain coupling is fundamental in unique functional properties of ferroelastic domain walls. Steep strain gradients through ferroelastic domain walls can interact independently with an order parameter, leading to physical properties that are quite distinct from those of domains themselves [4,7–10].

Cu_2OSeO_3 is an important model system in understanding strain coupling associated with magnetic ordering. It exhibits multiple magnetic phases in response to temperature and magnetic-field variations below the transition temperature of $T_c \sim 60$ K [11–15]. Competition between the symmetric exchange interaction and the antisymmetric Dzyaloshinskii-Moriya interaction stabilizes a helical ground state with a modulation period of ~ 50 – 70 nm. The propagation vectors of helices are parallel to any one of the (100) directions in each of multiple domains. Above a first critical magnetic field, the helical structure transforms into a single domain

^{*}kadachi@iwate-u.ac.jp

conical structure where magnetic moments precess around the direction of the magnetic field. The conical structure then turns into a field-polarized collinear ferrimagnetic structure above a second critical value. Its ferrimagnetism originates from clusters of four Cu ions in which one Cu^{2+} moment at the $4a$ site is antiparallel to three Cu^{2+} moments at the $12b$ site [11,16–18]. Helices in the ground state are also composed of ferrimagnetic spin clusters [19]. Chauhan *et al.* [13] identified a fluctuation disordered phase in a temperature interval of ~ 1 K immediately below the transition point. The most interesting aspect of the magnetic structures of Cu_2OSeO_3 is the skyrmion lattice [20,21], which emerges in a narrow temperature and magnetic field range near T_c . In contrast to other skyrmion host B20 compounds such as MnSi and FeGe, Cu_2OSeO_3 is an insulating material that displays magnetoelectric coupling, leading to distinctive properties of skyrmions [15,22–25].

A particular feature of Cu_2OSeO_3 is the lack of symmetry-breaking strain accompanying the paramagnetic to ferrimagnetic transition [16,17,26–28]. The development of ferrimagnetic order requires lowering of the symmetry from a paramagnetic cubic structure (space group $P2_13$) to a rhombohedral structure (space group $R3$) because ferrimagnetism is incompatible with cubic magnetic symmetry [16]. Recent powder x-ray diffraction data have revealed a small volume strain accompanying the magnetic transition at ~ 60 K in zero field but no evidence for a measurable distortion from cubic lattice geometry [28]. Furthermore, there appear to be no reports of the presence of ferroelastic twinning that would be indicative of a change to rhombohedral lattice geometry. Macroscopic electric polarization in Cu_2OSeO_3 arises only in the presence of a magnetic field and does not lead to switching in response to an electric field [16,18,20,29], indicating that it is not ferroelectric. This may also be an effect of having a negligibly small rhombohedral shear strain.

Evans *et al.* [27] confirmed that while any magnetoelectric coupling in Cu_2OSeO_3 is weak, it indeed gives rise to small but measurable changes in elastic properties at some of the known magnetic transitions. They used resonant ultrasound spectroscopy (RUS) to map out the distribution of elastic anomalies as functions of both temperature and magnetic field across the stability fields of the main magnetic structures observed with magnetic field along [111]. There were obvious anomalies at the first transition from the paramagnetic structure with falling temperature and the final conical-collinear transition with increasing field. Other smaller anomalies were observed in the elastic properties but were not so clearly related to boundaries between different magnetic structures. Elastic properties associated with the formation of the skyrmion lattice were not examined.

Evans *et al.* [27] investigated the overall elastic and anelastic behavior of Cu_2OSeO_3 , focusing on a temperature-magnetic field region well below T_c . In contrast, the primary objective of the present study was to investigate strain coupling with the skyrmion lattice in Cu_2OSeO_3 by collecting detailed RUS data in a dense region of magnetic phases near T_c . Qian *et al.* [12] showed that the stability field of the skyrmion phase has diffuse boundaries, whose location

depends on the technique and criteria used to identify them. The precise boundaries may also depend on the magnetothermal history of the sample in terms of varying temperature, field, or both together. The transition between the skyrmion and conical phases occurs through their coexistence region [30,31]. The coexistence of skyrmions within a different magnetic phase generally results in a glassy state, as has been observed in various skyrmion host compounds [12,32–35]. The RUS results obtained in the present paper characterize the glassy behavior of skyrmions in terms of strain coupling. They provide not only complementary information for the results of Evans *et al.* [27] but also insights into the elastic and anelastic behavior associated with magnetic ordering in Cu_2OSeO_3 .

II. EXPERIMENTAL DETAILS

The same Cu_2OSeO_3 single crystal as used in the study of Evans *et al.* [27] was used for the present paper. Because it has a very low intrinsic loss, even the most subtle changes in acoustic resonance frequencies, relating to single crystal elastic moduli, and acoustic loss can be identified with confidence. The measurement of these acoustic properties involves, in effect, the application of dynamic stress and observation of the strain response of the crystal. As such, the results of acoustic measurement should provide complementary information for characterizing relaxations observed in ac magnetic measurements, where the dynamic field is magnetic and the response of the crystal is determined by magnetic susceptibility and magnetic loss.

The RUS technique has been described in detail elsewhere [36–41]. The method involves measuring the resonant response of samples, which provides insights into elastic and anelastic properties. In a typical experimental arrangement, a sample is held lightly between piezoelectric transducers across opposite corners or opposite faces. Acoustic vibrations of the sample are generated and detected by each of the transducers. Sweeping the frequency of the driving transducer through a given range results in a resonance spectrum, where resonance peaks are observed corresponding to vibrational eigenmodes of the sample. Facilities in Cambridge allow resonance spectra to be collected in low-temperature and magnetic field environments [42]. The measurement system was developed by incorporating a plastic RUS head [43] into an Oxford Instruments Teslatron PT cryostat equipped with a 14-T superconducting solenoid magnet.

The Cu_2OSeO_3 crystal has an irregular polygon shape with a pair of growth faces parallel to $\{111\}$. As shown in Fig. 1(a), the sample was held lightly between piezoelectric transducers across the well-defined faces such that an applied magnetic field was exactly along [111]. The sample chamber was filled with 1 bar of helium gas at room temperature to facilitate thermal exchange. Resonance spectra were collected in automated sequences of varying temperature in a constant magnetic field or varying field at constant temperature. The trajectories of the RUS experiments performed in the present paper are shown superimposed on the phase diagram of Chauhan *et al.* [13] in Fig. 2. The variable temperature ranged from 30 to 80 K with a cooling rate of ~ 0.1 K/min, and its step varied from 0.1 to 2 K depending on the perceived proximity of magnetic phase

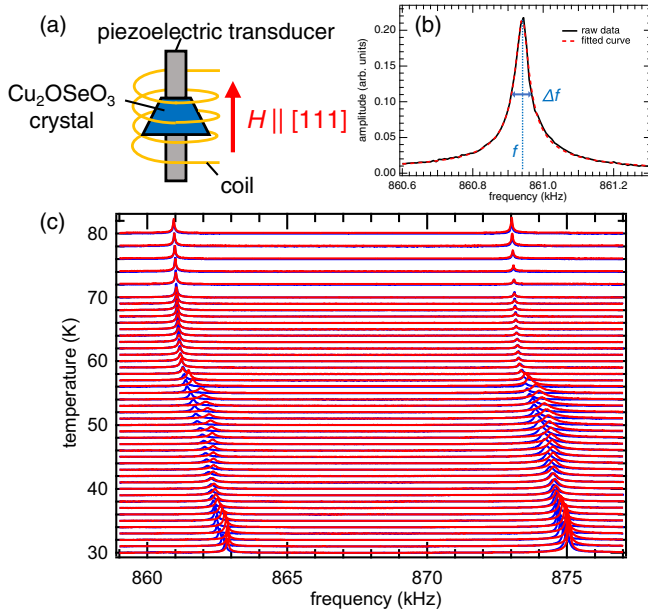


FIG. 1. (a) Schematic of the measurement setup for RUS experiments in low-temperature and magnetic-field environments. (b) An example of the asymmetric Lorentzian curve fit to a resonance peak, providing the peak frequency, f , and width at half maximum height, Δf , of the peak. (c) Segments of RUS spectra collected from the single crystal of Cu_2OSeO_3 during cooling (blue lines), followed by heating (red lines) in a 25 mT field. The y axis is really the amplitude from the amplifier but the spectra are stacked in proportion to the temperature at which they were collected; the axis was then relabeled as temperature to allow easy visualization of the evolution of individual resonance peaks with decreasing and increasing temperature.

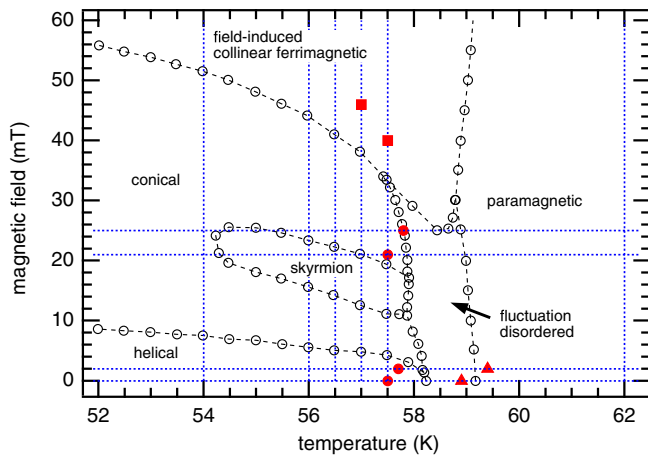


FIG. 2. Magnetic phase diagram of Cu_2OSeO_3 in the vicinity of the transition temperature (after Chauhan *et al.* [13]). Blue dotted lines show the trajectories along which RUS spectra were collected with variable temperature at constant field or variable field at constant temperature. Filled circles mark the upper temperature limit of hysteresis in f^2 values between heating and cooling. Filled triangles represent the temperature at which small anomalies in f^2 and Q^{-1} occur in zero field and in a 2 mT field. Filled squares show the upper magnetic field limit of hysteresis in f^2 values between increasing and decreasing fields.

transitions. The sequence of data collection with variable field consisted of increasing followed by decreasing magnetic field in 1 mT steps between 0 and 60 mT. When a sequence of increasing and decreasing field was carried out, the sample was heated to 70 K to leave no effects of magnetic hysteresis between experiments. A settle time at each set point before data collection was set to 15 min or 5 min when varying temperature or magnetic field, respectively. Each spectrum consisted of 65 000 data points in the frequency range 400–1600 kHz.

Resonance spectra were analyzed using the software package IGOR PRO (Wavemetrics). The peak frequency, f , and width at half maximum height, Δf , of each resonance peak were obtained by fitting an asymmetric Lorentzian function [Fig. 1(b)]. The irregular shape of the Cu_2OSeO_3 crystal prevented us from determining absolute values of the elastic constants via conventional inverse calculation. Changes in elastic properties were therefore characterized in terms of the variations of f^2 for individual peaks, which scale with different combinations of elastic constants (depending on the particular distortions involved in each resonance mode). The anelastic property was evaluated in terms of the inverse mechanical quality factor, $Q^{-1} = \Delta f/f$ [36,39,44].

III. RESULTS

Figure 1(c) contains a stack of segments of resonance spectra collected in a sequence of cooling followed by heating at 25 mT. The temperature dependence of resonance peak frequencies shows a significant change in trend at ~ 60 K, below which the evolution of the frequencies displays a clear hysteresis between cooling and heating. Peak broadening, corresponding to increase in Q^{-1} values, was also discernible below ~ 70 K. Figure 3 shows the variations of f^2 and Q^{-1} for selected peaks in the resonance spectra collected in a 25 mT field. Figure 4 presents f^2 and Q^{-1} data for a representative resonance near 1017 kHz, which demonstrates a significant loss peak at ~ 60 K, measured as a function of temperature in fields of 0, 2, and 21 mT. It can be seen in Figs. 3 and 4 that the evolution of f^2 in fields of 0, 2, 21, and 25 mT showed marked hysteresis below an upper temperature limit of ~ 57.5 , 57.7, 57.5, and 57.8 K, respectively. Values of the upper temperature limit are ~ 2 K below the temperature at which a change in slope occurs and, as shown in Fig. 2, appear to lie just below the lower stability limit of the fluctuation disordered phase in the phase diagram of Chauhan *et al.* [13]. However, there do not appear to be any obvious anomalies in f^2 that could be related specifically to the stability field of the skyrmion lattice.

The temperature dependence of the peak broadening shown in Fig. 1(c) can be characterized by three peaks in Q^{-1} , centered at ~ 40 , ~ 50 , and ~ 60 K (Fig. 3). The loss peak at ~ 40 K showed no hysteresis in the peak temperature, whereas the other loss peaks showed hysteresis, where the peak temperature appears to be slightly higher during heating compared with cooling. The magnitude of the loss peaks varied substantially between resonances, implying that related loss processes are sensitive to strain components involved in each resonance mode. The maximum values of Q^{-1} were less

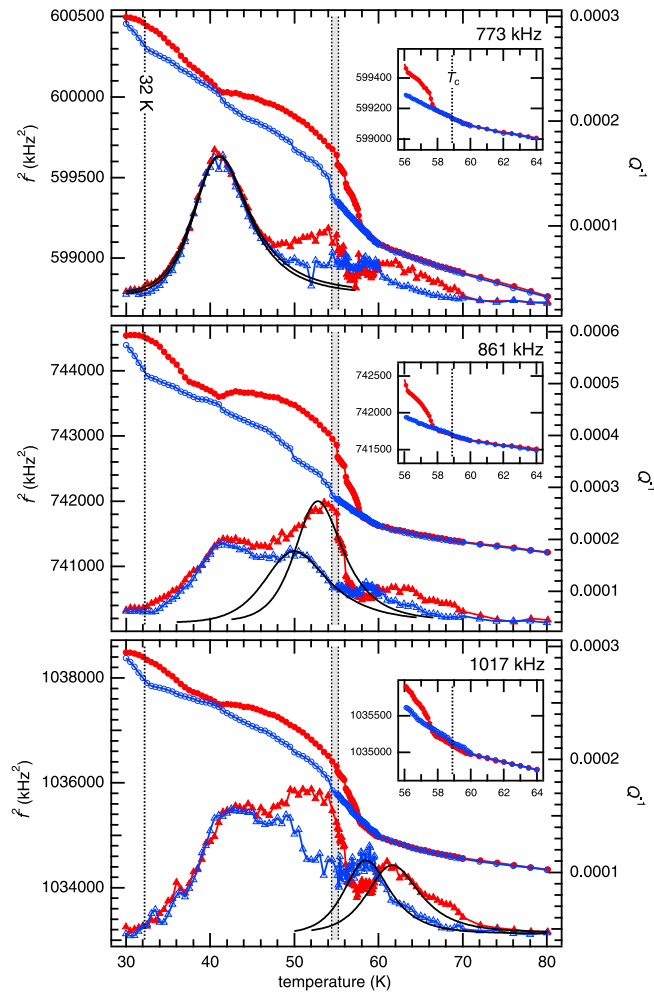


FIG. 3. Variations of f^2 and Q^{-1} for resonances near 773, 861, and 1017 kHz in the RUS spectra collected at 25 mT. Filled symbols = heating; open symbols = cooling. Insets show details of f^2 variations in the vicinity of T_c . Vertical dotted lines at 32 K mark the helical-conical transition temperature reported by Adams *et al.* [11]. Shaded areas indicate the expected stability field of the skyrmion lattice [13]. Black curves are fits of Eq. (1) to Debye-like peaks in Q^{-1} .

than ~ 0.0003 , reflecting low intrinsic acoustic loss of the crystal.

A Debye-like peak in Q^{-1} observed in RUS measurements made as a function of temperature, T , can be described by [3,45]

$$Q^{-1}(T) = Q_m^{-1} \left[\cosh \left\{ \frac{E_a}{Rr_2(\beta)} \left(\frac{1}{T} - \frac{1}{T_m} \right) \right\} \right]^{-1}, \quad (1)$$

where R is the gas constant. The acoustic dissipation has a maximum value, Q_m^{-1} , at T_m with the condition $\omega\tau = 1$, where ω is the angular frequency of an applied stress and τ is the relaxation time for a thermally activated process responsible for the acoustic dissipation. The temperature dependence of Q^{-1} is characterized by an activation energy, E_a , and a parameter that defines the width of a Gaussian distribution of relaxation times, $r_2(\beta)$. Figure 3 gives an example of fitting of Eq. (1) to Debye-like loss peaks. Fits to the loss peak at

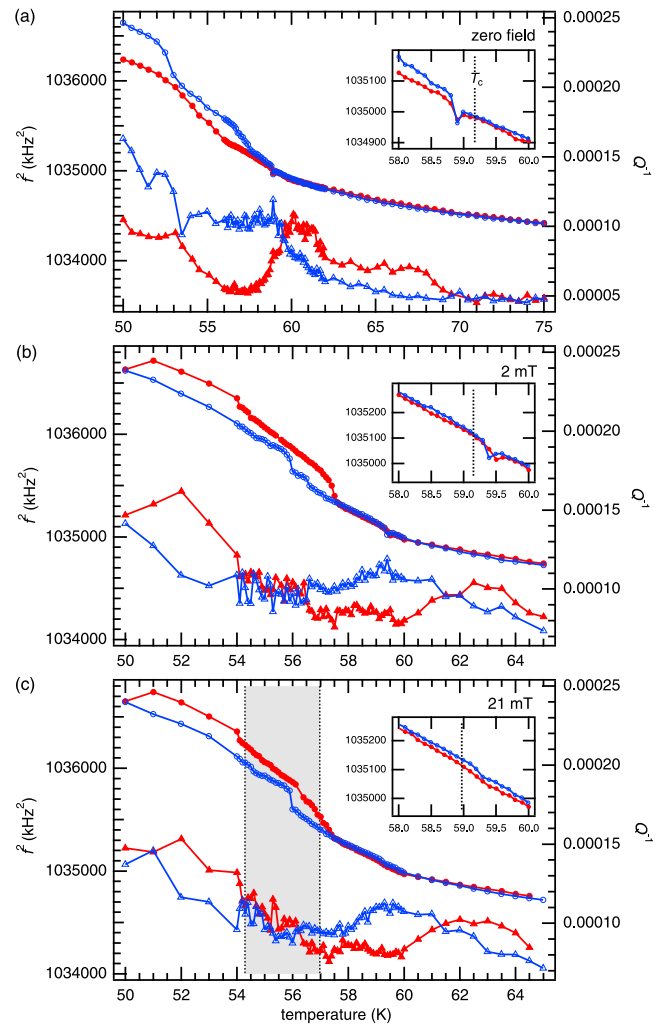


FIG. 4. Variations of f^2 and Q^{-1} for a resonance near 1017 kHz in RUS spectra collected during a sequence of heating followed by cooling in zero field (a) and during a sequence of cooling followed by heating in 2 mT (b) and 21 mT (c) fields. Filled symbols = heating; open symbols = cooling. Insets are expanded sections of the f^2 variation in the vicinity of T_c , demonstrating the presence of a small but distinct dip. Shaded area indicates the expected stability field of the skyrmion lattice [13].

~ 40 K for selected resonances in the RUS spectra collected during cooling in a 25 mT field revealed a typical frequency dependence of T_m [Fig. 5(a)]. An Arrhenius plot of the result [Fig. 5(b)] yielded an activation energy of 49 ± 7 meV.

In zero field and in a 2 mT field, there are small anomalies in f^2 and Q^{-1} which imply some acoustic loss process (Fig. 6). The pattern does not match the classic pattern of Debye freezing, but the temperature at which the anomaly is observed, ~ 59 K, coincides exactly with the onset of the stability field of the fluctuation disordered phase (Fig. 2). This suggests that some dynamical magnetic process couples weakly with strain and has a temperature-dependent frequency that crosses the frequency of acoustic resonances of the crystal at ~ 59 K to cause slight attenuation. The same effect is not seen at 21 and 25 mT, presumably because the dynamical process is suppressed by the magnetic field or

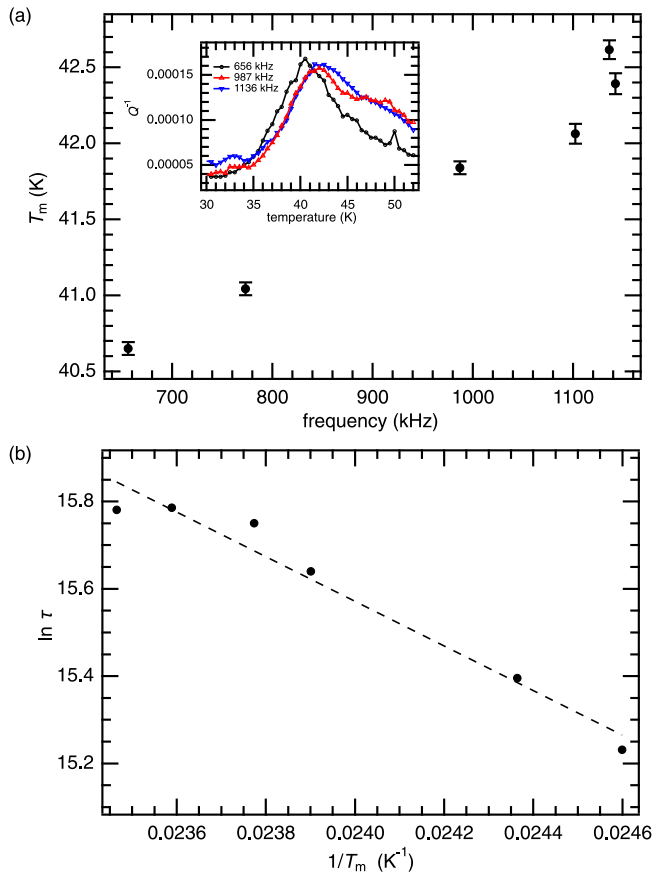


FIG. 5. (a) Values of T_m determined from fitting of a loss peak at ~ 40 K in the Q^{-1} data from selected resonances collected during cooling in a 25 mT field. The inset shows details of Q^{-1} variations of representative resonances. Arrhenius plot is shown in (b), where the slope of the straight line fit gives activation energy of 49 ± 7 meV.

has frequencies which become significantly different from ~ 1 MHz in an applied field.

Figure 7 compares variations of f^2 for two representative resonances measured as a function of magnetic field at six different temperatures. None of the corresponding data for Q^{-1} showed any anomalies or hysteresis. f^2 values were the same between increasing and decreasing fields at 54 and 62 K, whereas they displayed marked hysteresis at the other temperatures. The hysteretic variations of f^2 passed through the stability field of the skyrmion lattice but there were no anomalies at the expected boundaries of this field. The trend of reducing f^2 values during the full sequence of increasing and decreasing field at 56 and 56.5 K resembles glassy behavior seen in other systems [46,47], where there appears to be a continuous drift in values with time rather than any systematic dependence on magnetic field; i.e., the system did not appear to achieve an equilibrium state. The upper field limit of the hysteresis at 57 and 57.5 K is ~ 46 mT and ~ 40 mT, respectively. These points fall close to the boundary between the stability fields of single domain conical and field-polarized collinear ferrimagnetic structures (Fig. 2). Evans *et al.* [27] also found distinct acoustic anomalies associated with this transition.

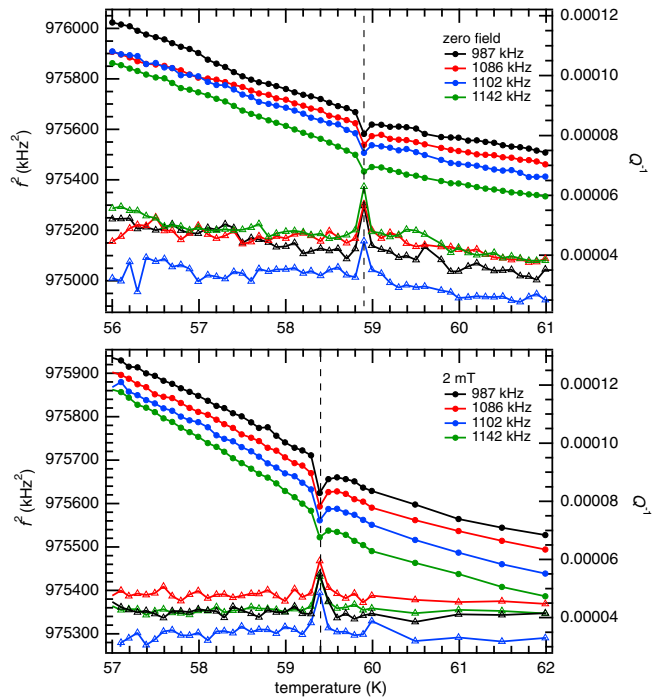


FIG. 6. Enhanced views of variations of f^2 and Q^{-1} for selected resonances in RUS spectra collected during cooling in zero field and in a 2 mT field. Step softening accompanied by a steep increase in acoustic loss is clearly seen in a narrow temperature interval close to 59 K.

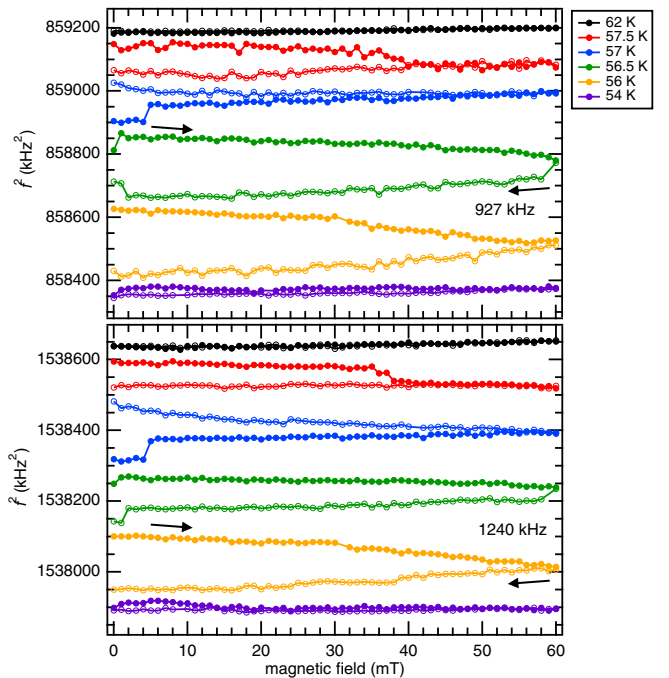


FIG. 7. Evolution of f^2 values for resonances near 927 and 1240 kHz as a function of increasing (filled symbols) and decreasing (open symbols) magnetic field at 54, 56, 56.5, 57, 57.5, and 62 K. f^2 values have been multiplied by arbitrary scaling factors to allow for easy comparison of the trends of f^2 with magnetic field at different temperatures. Arrows indicate the direction of time evolution of the experiment.

IV. DISCUSSION

A. Variation of f^2 as a function of temperature at constant field

All the f^2 data collected as a function of temperature at constant field show a change in slope at ~ 60 K, consistent with the RUS measurements by Evans *et al.* [27]. It coincides exactly with the onset of steep increase in magnetic susceptibility reported in the literature [12,13,19,28,48]. This confirms the existence of magnetoelastic coupling, i.e., coupling between strain and the magnetic order parameter. No symmetry-breaking shear strain has yet been observed by diffraction methods, but the lattice parameter data of Dutta *et al.* [28] show that the paramagnetic–ferrimagnetic transition in zero field is accompanied by a small positive volume strain with magnitude of up to ~ 0.0006 . In combination with the analysis of strain coupling by Evans *et al.* [27], the implication is that the change in the overall trend of f^2 with falling temperature is determined by biquadratic strain coupling of the form $\lambda e_a^2 M^2$, where λ is the coupling coefficient, e_a is the volume strain, and M is the magnetic order parameter.

Differences in elastic moduli in the temperature interval ~ 41 – 58 K (Fig. 3) imply that some aspects of the microstructure evolve with falling temperature in a manner that is different from their evolution with increasing temperature. The elastic moduli would not change with changing magnetic domain sizes and configurations, however, because there is no overt strain contrast between domains. A possible explanation might be that the domains are locally piezomagnetic and/or piezoelectric [27]. If this is the case, changing the proportions of different domain orientations could result in changes in the effective piezo coefficients of the bulk sample which, in turn, would contribute to small changes in the resonance frequencies, as in the case of ϵ -Fe₂O₃ [47]. Differences in the magnitude of the hysteresis between resonances may be explained by the fact that piezoelectric and piezomagnetic coefficients, as with elastic constants, contribute to each resonance frequency in different proportions.

Another possible explanation for the hysteretic variations of f^2 might be the metastable skyrmion lattice [49,50]. However, the condition of the present RUS experiments, that is, relatively slow cooling rate with an applied magnetic field along [111] is unfavorable for the formation of metastable skyrmions [24,51]. In addition, the metastable skyrmion lattice is unlikely to be responsible for the difference in f^2 values between heating and cooling because this hysteresis was seen even in zero field and in a 2 mT field [Figs. 4(a) and 4(b)], where the trajectories of the experiments do not pass through the stability field of the skyrmion phase.

Hysteresis in the evolution of f^2 below 40 K in Fig. 3 is most likely related to the helical–conical transition, whose transition temperature is ~ 32 K at 25 mT [11]. Breaks in slope at 32.5 K on cooling and 37.5 K on heating appear to correspond to the transition point and are most likely related to elastic softening as the transition point is approached from below, which is typical for elastic anomalies associated with a magnetic phase transition [52–55]. The difference in the transition point between heating and cooling suggests first-order character, consistent with a first-order transition between the helical and conical phases through a metamagnetic phase

below 50 K reported by Chauhan *et al.* [14]. However, there is no overt discontinuity in f^2 at the transition point for all the resonances, implying that the helical–conical transition with variable temperature involves only very weak coupling with strain.

In addition to the hysteretic variations, the evolution of f^2 in 21 and 25 mT fields shows small discontinuities at different temperatures during heating and cooling. The temperatures at which the discontinuities occur fall close to the boundary of the stability field of the skyrmion lattice shown in the phase diagram of Chauhan *et al.* [13]. A similar feature is seen in the cooling sequence at 2 mT [Fig. 4(b)]. The discontinuities most likely arise from changes in microstructures due to jerky movements of domain walls which are otherwise immobile. The magnitudes of the discontinuities are approximately the same as or slightly less than the differences between hysteretic values observed during heating and cooling over wider temperature intervals. While a firm explanation cannot be offered without a more detailed understanding of the microstructure involved, these findings suggest that elastic depinning of some weakly pinned domain structures occurs below the temperature at which hysteretic evolution occurs.

Data for f^2 and Q^{-1} collected at 2 and 21 mT in the same temperature interval and steps showed a quite similar pattern of variations [Figs. 4(b) and 4(c)]. Comparison of the f^2 data highlights the only difference between them seen in the temperature interval ~ 56 – 58 K on heating (Fig. 8). This interval coincides with the stability field of the skyrmion phase in a 21 mT field shown in the phase diagram of Adams *et al.* [11] with field parallel to [111]. The implication is that the difference in f^2 values could be attributed to differences in elasticity between the helical and skyrmion phases. Lower values of f^2 in 21 mT field show that the skyrmion phase is slightly softer than the helical phase on heating, implying that differences in elastic moduli can demarcate the boundaries of the stability field of the skyrmion phase. The observation that the difference in elasticity between the skyrmion and helical phases is barely detectable on cooling suggests that

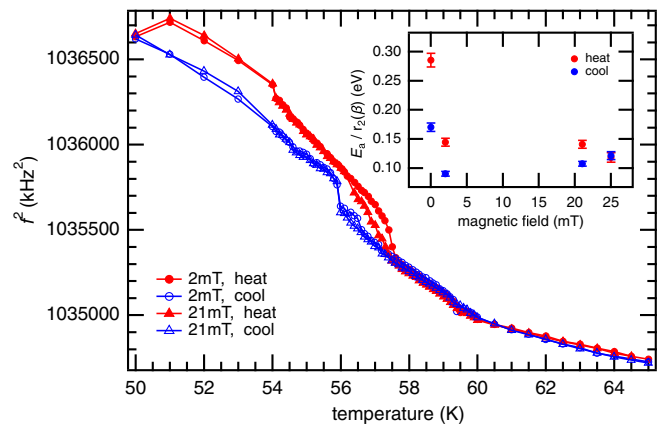


FIG. 8. Comparison of f^2 data for a resonance near 1017 kHz in a 2 mT field and in a 21 mT field shown in Fig. 4. Inset shows values of $E_a/r_2(\beta)$ in four different magnetic fields determined from fitting of a peak in Q^{-1} at ~ 60 K for this resonance.

the elastic properties of the skyrmion phase are sensitive to thermal history. The f^2 data collected at 2 and 21 mT were indistinguishable from each other below 56 K (Fig. 8), indicating that the elasticity of the helical phase is identical to that of the conical phase.

B. Variation of Q^{-1} as a function of temperature at constant field

As discussed by Evans *et al.* [27], the peak in Q^{-1} at ~ 40 K is accompanied by slight stiffening with falling temperature in a manner that is diagnostic of Debye-like freezing. They showed that application of a magnetic field up to 220 mT causes no change in the loss peak, implying that the loss process does not involve magnetic relaxations. Similarly, there appears to be no comparable loss peak in ac magnetic data. The acoustic loss might be extrinsic due to freezing of defects or intrinsic due to freezing of some dynamic aspects of the microstructure. Whatever the loss mechanism is, it is not changed by application of magnetic field. Evans *et al.* [27] obtained the value of $E_a/r_2(\beta)$ by fitting to the peak in Q^{-1} for a resonance near 1104 kHz. Assuming that the loss mechanism had a single relaxation time ($r_2(\beta) = 1$), they estimated the activation energy to be ~ 55 meV. The activation energy of ~ 50 meV obtained from the Arrhenius plot [Fig. 5(b)] is the same within realistic experimental uncertainty, confirming that the loss process is indeed determined by a single relaxation time. Although an underlying cause of the Debye-like freezing has not been defined, it is most likely to be responsible for a close agreement between the values of f^2 obtained during heating and cooling in the vicinity of 40 K (Fig. 3). This suggests that the freezing process involves some structural memory effects that lead to a particular microstructure independently of thermal history.

The high-resolution RUS data have revealed a series of overlapping acoustic loss peaks at temperatures between ~ 50 and ~ 65 K. These peaks have been analyzed in most detail using resonance peaks in the data collected at 25 mT (Fig. 3). The fact that different resonance peaks show different variations in Q^{-1} implies that the mechanism responsible for the losses has different coupling strengths with different strains. There is no independent evidence for the loss mechanism, but fitting Eq. (1) to the peak in Q^{-1} at ~ 50 K for a resonance near 861 kHz gave values for $E_a/r_2(\beta)$ of 94 and 64 meV on heating and cooling, respectively. Similar analyses of the 60 K loss peak revealed a significant difference between the presence and absence of magnetic field (Fig. 8), indicating that the predominant effect of the complete transition from paramagnetic to skyrmion lattice or single domain conical structures involves freezing of some dynamic aspect(s) of the magnetic structure. A possible loss mechanism may be pinning of magnetic topological defects, for which the activation energy has been reported as ~ 0.1 eV [35].

AC magnetic data of Levatic *et al.* [56] showed that there is no magnetic loss in zero field, and magnetic loss behavior in the vicinity of T_c has a strong dependence on the strength of an applied dc magnetic field. These features differ from those of acoustic loss behavior near 60 K (Figs. 3 and 4). Qian *et al.* [12] observed ac magnetic loss peaks as a function of field, in contrast with the featureless behavior of Q^{-1} seen by RUS.

These discrepancies are indicative of weak magnetoelastic coupling of Cu_2OSeO_3 .

The data for f^2 and Q^{-1} measured as a function of temperature show strain effects which appear to demarcate the boundaries of the stability field of the fluctuation disordered phase. There is a break in slope of f^2 at ~ 60 K, which has been attributed to the development of some form of magnetic order with weak magnetoelastic coupling. The evolution of f^2 is fully reversible between heating and cooling in the temperature interval ~ 58 – 60 K (Figs. 3 and 4). The onset of the multidomain helical, single-domain conical, and skyrmion lattice structures at ~ 58 K appears to be marked by freezing processes that give rise to both magnetic loss [12,56] and acoustic loss with distinct hysteresis. The simplest interpretation is that any microstructure, such as magnetic topological defects, is mobile in the fluctuation disordered region but pinned in the multidomain helical, single-domain conical, and skyrmion lattice structures.

C. Variation of f^2 as a function of field at constant temperature

Measurable changes in elastic properties occurred at the transition from the single-domain conical to field-polarized collinear ferrimagnetic structures, as seen also by Evans *et al.* [27]. This transition, at least, gives rise to sufficient static strain coupling that results in changes to the single crystal elastic moduli. As shown in Fig. 7, the f^2 data collected at 56.5 and 57 K displayed small discontinuities at ~ 2 and ~ 4 mT, which fall close to the boundary between the stability fields of the multidomain helical and single-domain conical structures. This is consistent with the RUS results of Evans *et al.* [27] in showing that there is a clear indication of strain relaxation accompanying the conical-collinear transition, while the helical-conical transition involves only some weaker and less regular strain-coupling effects.

The absence of obvious anomalies in f^2 associated with the helical-conical transition when varying fields at constant temperature contrasts with the observation of elastic softening as the transition temperature is approached from below (Fig. 3). This suggests that a driving mechanism for the helical-conical transition is different between varying temperatures at constant field and varying fields at constant temperature. Driving mechanisms for other phase transitions in Cu_2OSeO_3 also likely depend on the way in which experiments are carried out. In fact, Qian *et al.* [12] reported that magnetic transitions into and out of the skyrmion phase with variable temperatures differ from those with variable fields.

D. Weak coupling of strain with skyrmion lattice

With respect to skyrmions, we can conclude that the skyrmion lattice is weakly pinned, if at all, by strain effects. It is notable that the apparent glassy pattern of evolution of f^2 with magnetic field at constant temperature only occurs in the temperature range where the skyrmion lattice forms (Fig. 7). This observation may support the hypothesis that the other magnetic structures become stable when the skyrmions can no longer move relatively freely, as in relaxation accompanied with formation of a glassy state. In this case, the transition sequence with falling temperature would be paramagnetic \rightarrow

mobile skyrmions or dynamical short range order \rightarrow static magnetic order.

The hypothesis that the skyrmions experience very low viscosity, i.e. with liquidlike behavior, appears to match up with the observations that skyrmions in metallic samples can be driven by much lower current density compared with magnetic domains [57,58] and dynamics of skyrmions tend to conform to the predictions of weak collective pinning theory [59]. Individual skyrmions in Cu_2OSeO_3 have widths of ~ 60 nm [20], which is significantly wider than ferroelastic twin walls. It is well-known that thin walls interact with point defects more strongly than thick walls, but the thickness of the thin twin walls tends to be only a few angstroms. In combination with intrinsically weak magnetoelastic coupling, the skyrmions with widths of 60 nm would interact extremely weakly with strain fields around point defects, resulting in glassy or liquidlike behavior. The RUS results reported here provide confirmation of this behavior and raise the question as to whether weak magnetoelastic coupling is a fundamental requirement for the formation of a skyrmion lattice.

V. CONCLUSIONS

The most obvious result is that, as found in previous RUS work [27], any anomalies in elastic and anelastic properties are small. This is consistent with the overall view that magnetoelastic coupling is weak and any strain effects are small. These RUS results provide additional evidence that the weak magnetoelastic coupling in Cu_2OSeO_3 causes measurable changes in elastic and anelastic properties. They can be a good criterion for demarcating the boundaries of the stability fields of the skyrmion and fluctuation disordered phases, which are generally quite diffuse. The measurements of elastic properties with variable fields suggest that skyrmions in Cu_2OSeO_3 show glassy or liquidlike behavior, consistent with their large size in comparison with twin walls and their extremely weak intrinsic magnetoelastic coupling. Knowledge of the variation of the elastic constants associated with magnetic phase transitions could contribute to our understanding of the strength and underlying mechanisms of strain coupling for Cu_2OSeO_3 and the potential manipulation of skyrmion functional properties through controlled strain fields.

-
- [1] M. A. Carpenter, E. K. H. Salje, and A. Graeme-Barber, Spontaneous strain as a determinant of thermodynamic properties for phase transitions in minerals, *Eur. J. Mineral.* **10**, 621 (1998).
- [2] M. A. Carpenter and E. K. H. Salje, Elastic anomalies in minerals due to structural phase transitions, *Eur. J. Mineral.* **10**, 693 (1998).
- [3] M. A. Carpenter, Static and dynamic strain coupling behaviour of ferroic and multiferroic perovskites from resonant ultrasound spectroscopy, *J. Phys.: Condens. Matter* **27**, 263201 (2015).
- [4] E. K. H. Salje and H. Zhang, Domain boundary engineering, *Phase Transitions* **82**, 452 (2009).
- [5] D. Meier, Functional domain walls in multiferroics, *J. Phys.: Condens. Matter* **27**, 463003 (2015).
- [6] G. F. Nataf, M. Guennou, J. M. Gregg, D. Meier, J. Hlinka, E. K. H. Salje, and J. Kreisel, Domain-wall engineering and topological defects in ferroelectric and ferroelastic materials, *Nat. Rev. Phys.* **2**, 634 (2020).
- [7] L. Goncalves-Ferreira, S. A. T. Redfern, E. Artacho, and E. K. H. Salje, Ferrielectric twin walls in CaTiO_3 , *Phys. Rev. Lett.* **101**, 097602 (2008).
- [8] Y. Kim, M. Alexe, and E. K. H. Salje, Nanoscale properties of thin twin walls and surface layers in piezoelectric WO_{3-x} , *Appl. Phys. Lett.* **96**, 032904 (2010).
- [9] J. F. Scott, E. K. H. Salje, and M. A. Carpenter, Domain wall damping and elastic softening in SrTiO_3 : Evidence for polar twin walls, *Phys. Rev. Lett.* **109**, 187601 (2012).
- [10] H. Yokota, S. Matsumoto, E. K. H. Salje, and Y. Uesu, Polar nature of domain boundaries in purely ferroelastic $\text{Pb}_3(\text{PO}_4)_2$ investigated by second harmonic generation microscopy, *Phys. Rev. B* **100**, 024101 (2019).
- [11] T. Adams, A. Chacon, M. Wagner, A. Bauer, G. Brandl, B. Pedersen, H. Berger, P. Lemmens, and C. Pfleiderer, Long-wavelength helimagnetic order and skyrmion lattice phase in Cu_2OSeO_3 , *Phys. Rev. Lett.* **108**, 237204 (2012).
- [12] F. Qian, H. Wilhelm, A. Aqeel, T. T. M. Palstra, A. J. E. Lefering, E. H. Bruck, and C. Pappas, Phase diagram and magnetic relaxation phenomena in Cu_2OSeO_3 , *Phys. Rev. B* **94**, 064418 (2016).
- [13] H. C. Chauhan, B. Kumar, J. K. Tiwari, and S. Ghosh, Multiple phases with a tricritical point and a Lifshitz point in the skyrmion host Cu_2OSeO_3 , *Phys. Rev. B* **100**, 165143 (2019).
- [14] H. C. Chauhan, B. Kumar, and S. Ghosh, Origin of metamagnetism in skyrmion host Cu_2OSeO_3 , *Sci. Rep.* **12**, 15971 (2022).
- [15] M. Crisanti, A. O. Leonov, R. Cubitt, A. Labh, H. Wilhelm, M. P. Schmidt, and C. Pappas, Tilted spirals and low-temperature skyrmions in Cu_2OSeO_3 , *Phys. Rev. Res.* **5**, 033033 (2023).
- [16] Jan-Willem G. Bos, C. V. Colin, and T. T. M. Palstra, Magnetolectric coupling in the cubic ferrimagnet Cu_2OSeO_3 , *Phys. Rev. B* **78**, 094416 (2008).
- [17] M. Belesi, I. Rousochatzakis, H. C. Wu, H. Berger, I. V. Shvets, F. Mila, and J. P. Ansermet, Ferrimagnetism of the magnetolectric compound Cu_2OSeO_3 probed by ^{77}Se NMR, *Phys. Rev. B* **82**, 094422 (2010).
- [18] V. P. Gnezdilov, K. V. Lamonova, Y. G. Pashkevich, P. Lemmens, H. Berger, F. Bussy, and S. L. Gnatchenko, Magnetolectricity in the ferrimagnetic Cu_2OSeO_3 : Symmetry analysis and Raman scattering study, *Low Temp. Phys.* **36**, 550 (2010).
- [19] K. J. A. Franke, P. R. Dean, M. C. Hatnean, M. T. Birch, D. D. Khalyavin, P. Manuel, T. Lancaster, G. Balakrishnan, and P. D. Hatton, Investigating the magnetic ground state of the skyrmion host material Cu_2OSeO_3 using long-wavelength neutron diffraction, *AIP Adv.* **9**, 125228 (2019).
- [20] S. Seki, X. Z. Yu, S. Ishiwata, and Y. Tokura, Observation of skyrmions in a multiferroic material, *Science* **336**, 198 (2012).
- [21] S. Seki, J.-H. Kim, D. S. Inosov, R. Georgii, B. Keimer, S. Ishiwata, and Y. Tokura, Formation and rotation of skyrmion

- crystal in the chiral-lattice insulator Cu_2OSeO_3 , *Phys. Rev. B* **85**, 220406(R) (2012).
- [22] J. S. White, K. Prsa, P. Huang, A. A. Omrani, I. Zivkovic, M. Bartkowiak, H. Berger, A. Magrez, J. L. Gavilano, G. Nagy, J. Zang, and H. M. Ronnow, Electric-field-induced skyrmion distortion and giant lattice rotation in the magnetoelectric insulator Cu_2OSeO_3 , *Phys. Rev. Lett.* **113**, 107203 (2014).
- [23] M. Mochizuki and S. Seki, Dynamical magnetoelectric phenomena of multiferroic skyrmions, *J. Phys.: Condens. Matter* **27**, 503001 (2015).
- [24] A. Chacon, L. Heinen, M. Halder, A. Bauer, W. Simeth, S. Muhlbauer, H. Berger, M. Garst, A. Rosch, and C. Pfleiderer, Observation of two independent skyrmion phases in a chiral magnetic material, *Nat. Phys.* **14**, 936 (2018).
- [25] S. Seki, M. Garst, J. Waizner, R. Takagi, N. D. Khanh, Y. Okamura, K. Kondou, F. Kagawa, Y. Otani, and Y. Tokura, Propagation dynamics of spin excitations along skyrmion strings, *Nat. Commun.* **11**, 256 (2020).
- [26] K. H. Miller, X. S. Xu., H. Berger, E. S. Knowles, D. J. Arenas, M. W. Meisel, and D. B. Tanner, Magnetodielectric coupling of infrared phonons in single-crystal Cu_2OSeO_3 , *Phys. Rev. B* **82**, 144107 (2010).
- [27] D. M. Evans, J. A. Schiemer, M. Schmidt, H. Wilhelm, and M. A. Carpenter, Defect dynamics and strain coupling to magnetization in the cubic helimagnet Cu_2OSeO_3 , *Phys. Rev. B* **95**, 094426 (2017).
- [28] P. Dutta, M. Das, A. Banerjee, S. Chatterjee, and S. Majumdar, Observation of structural anomaly and low-field magnetocaloric effect in Cu_2OSeO_3 , *J. Alloys Compd.* **886**, 161198 (2021).
- [29] E. Ruff, P. Lunkenheimer, A. Loidl, H. Berger, and S. Krohns, Magnetoelectric effects in the skyrmion host material Cu_2OSeO_3 , *Sci. Rep.* **5**, 15025 (2015).
- [30] T. Reimann, A. Bauer, C. Pfleiderer, P. Boni, P. Trtik, A. Tremsin, M. Schulz, and S. Muhlbauer, Neutron diffractive imaging of the skyrmion lattice nucleation in MnSi, *Phys. Rev. B* **97**, 020406(R) (2018).
- [31] Y. Chai, P. Lu, H. Du, J. Shen, Y. Ma, K. Zhai, L. Wang, Y. Shi, H. Li, W. Wang, and Y. Sun, Probe of skyrmion phases and dynamics in MnSi via the magnetoelectric effect in a composite configuration, *Phys. Rev. B* **104**, L100413 (2021).
- [32] P. Milde, D. Kohler, J. Seidel, L. M. Eng, A. Bauer, A. Chacon, J. Kindervater, S. Muhlbauer, C. Pfleiderer, S. Buhbrandt, C. Schütte, and A. Rosch, Unwinding of a skyrmion lattice by magnetic monopoles, *Science* **340**, 1076 (2013).
- [33] X. Yu, A. Kikkawa, D. Morikawa, K. Shibata, Y. Tokunaga, Y. Taguchi, and Y. Tokura, Variation of skyrmion forms and their stability in MnSi thin plates, *Phys. Rev. B* **91**, 054411 (2015).
- [34] J. Rajeswari, P. Huang, G. F. Mancini, Y. Murooka, T. Latychevskaia, D. McGrouther, M. Cantoni, E. Baldini, J. S. White, A. Magrez, T. Giamarchi, H. M. Ronnow, and F. Carbone, Filming the formation and fluctuation of skyrmion domains by cryo-Lorentz transmission electron microscopy, *Proc. Natl. Acad. Sci.* **112**, 14212 (2015).
- [35] A. Butykai, S. Bordacs, L. F. Kiss, B. G. Szigeti, V. Tsurkan, A. Loidl, and I. Kezsmarki, Relaxation dynamics of modulated magnetic phases in the skyrmion host GaV_4S_8 : An ac magnetic susceptibility study, *Phys. Rev. B* **96**, 104430 (2017).
- [36] A. Migliori, J. L. Sarrao, W. M. Visscher, T. M. Bell, M. Lei, Z. Fiskl, and R. G. Leisure, Resonant ultrasound spectroscopic techniques for measurement of the elastic moduli of solids, *Phys. B: Condens. Matter* **183**, 1 (1993).
- [37] J. Maynard, Resonant ultrasound spectroscopy, *Phys. Today* **49**(1), 26 (1996).
- [38] A. Migliori and J. L. Sarrao, *Resonant Ultrasound Spectroscopy: Applications to Physics, Materials Measurements, and Nondestructive Evaluation* (Wiley, New York, 1997).
- [39] R. G. Leisure and F. A. Willis, Resonant ultrasound spectroscopy, *J. Phys.: Condens. Matter* **9**, 6001 (1997).
- [40] R. G. Leisure, K. Foster, J. E. Hightower, and D. S. Agosta, Internal friction studies by resonant ultrasound spectroscopy, *Mater. Sci. Eng. A* **370**, 34 (2004).
- [41] F. F. Balakirev, S. M. Ennaceur, R. J. Migliori, B. Maiorov, and A. Migliori, Resonant ultrasound spectroscopy: The essential toolbox, *Rev. Sci. Instrum.* **90**, 121401 (2019).
- [42] J. Schiemer, L. J. Spalek, S. S. Saxena, C. Panagopoulos, T. Katsufuji, A. Bussmann-Holder, J. Kohler, and M. A. Carpenter, Magnetic field and in situ stress dependence of elastic behavior in EuTiO_3 from resonant ultrasound spectroscopy, *Phys. Rev. B* **93**, 054108 (2016).
- [43] R. E. A. McKnight, M. A. Carpenter, T. W. Darling, A. Buckley, and P. A. Taylor, Acoustic dissipation associated with phase transitions in lawsonite, $\text{CaAl}_2\text{Si}_2\text{O}_7(\text{OH})_2 \cdot \text{H}_2\text{O}$, *Am. Mineral.* **92**, 1665 (2007).
- [44] R. G. Leisure, *Ultrasonic Spectroscopy: Applications in Condensed Matter Physics and Materials Science* (Cambridge University Press, Cambridge, 2017).
- [45] M. Weller, G. Y. Li, J. X. Zhang, T. S. Ke, and J. Diehl, Accurate determination of activation enthalpies associated with the stress-induced migration of oxygen or nitrogen in tantalum and niobium, *Acta Metall.* **29**, 1047 (1981).
- [46] D. Pesquera, M. A. Carpenter, and E. K. H. Salje, Glasslike dynamics of polar domain walls in cryogenic SrTiO_3 , *Phys. Rev. Lett.* **121**, 235701 (2018).
- [47] C. R. S. Haines, M. Gich, J. L. Garcia-Munoz, A. Romaguera, Z. Ma, M. B. Costa, and M. A. Carpenter, Magnetoelastic coupling behaviour of nanocrystalline $\epsilon\text{-Fe}_2\text{O}_3$, *J. Magn. Mater.* **583**, 170240 (2023).
- [48] I. Levatic, P. Popcevic, V. Suriya, A. Kruchkov, H. Berger, A. Magrez, J. S. White, H. M. Ronnow, and I. Zivkovic, Dramatic pressure-driven enhancement of bulk skyrmion stability, *Sci. Rep.* **6**, 21347 (2016).
- [49] Y. Okamura, F. Kagawa, S. Seki, and Y. Tokura, Transition to and from the skyrmion lattice phase by electric fields in a magnetoelectric compound, *Nat. Commun.* **7**, 12669 (2016).
- [50] M. T. Birch, R. Takagi, S. Seki, M. N. Wilson, F. Kagawa, A. Stefancic, G. Balakrishnan, R. Fan, P. Steadman, C. J. Ottley, M. Crisanti, R. Cubitt, T. Lancaster, Y. Tokura, and P. D. Hatton, Increased lifetime of metastable skyrmions by controlled doping, *Phys. Rev. B* **100**, 014425 (2019).
- [51] L. J. Bannenberg, H. Wilhelm, R. Cubitt, A. Labh, M. P. Schmidt, E. Lelievre-Berna, C. Pappas, M. Mostovoy, and A. O. Leonov, Multiple low-temperature skyrmionic states in a bulk chiral magnet, *npj Quantum Mater.* **4**, 11 (2019).
- [52] R. I. Thomson, T. Chatterji, and M. A. Carpenter, CoF_2 : A model system for magnetoelastic coupling and elastic softening mechanisms associated with paramagnetic \leftrightarrow antiferromagnetic phase transitions, *J. Phys.: Condens. Matter* **26**, 146001 (2014).

- [53] M. A. Carpenter, D. M. Evans, J. A. Schiemer, T. Wolf, P. Adelman, A. E. Böhmer, C. Meingast, S. E. Dutton, P. Mukherjee, and C. J. Howard, Ferroelasticity, anelasticity and magnetoelastic relaxation in Co-doped iron pnictide: $\text{Ba}(\text{Fe}_{0.957}\text{Co}_{0.957})_2\text{As}_2$, *J. Phys.: Condens. Matter* **31**, 155401 (2019).
- [54] M. A. Carpenter, D. Pesquera, D. O'Flynn, G. Balakrishnan, N. Mufti, A. A. Nugroho, T. T. M. Palstra, M. Mihalik, M. Mihalik, M. Zentkova, A. Almeida, J. A. Moreira, R. Vilarinho, and D. Meier, Strain relaxation dynamics of multiferroic orthorhombic manganites, *J. Phys.: Condens. Matter* **33**, 125402 (2021).
- [55] C. M. Fernandez-Posada, C. R. S. Haines, D. M. Evans, Z. Yan, E. Bourret, D. Meier, and M. A. Carpenter, Magnetoelastic properties of multiferroic hexagonal ErMnO_3 , *J. Magn. Magn. Mater.* **554**, 169277 (2022).
- [56] I. Levatic, V. Surija, H. Berger, and I. Zivkovic, Dissipation processes in the insulating skyrmion compound Cu_2OSeO_3 , *Phys. Rev. B* **90**, 224412 (2014).
- [57] F. Jonietz, S. Mühlbauer, C. Pfleiderer, A. Neubauer, W. Münzer, A. Bauer, T. Adams, R. Georgii, P. Boni, R. A. Duine, K. Everschor, M. Garst, and A. Rosch, Spin transfer torques in MnSi at ultralow current densities, *Science* **330**, 1648 (2010).
- [58] T. Schulz, R. Ritz, A. Bauer, M. Halder, M. Wagner, C. Franz, C. Pfleiderer, K. Everschor, M. Garst, and A. Rosch, Emergent electrodynamics of skyrmions in a chiral magnet, *Nat. Phys.* **8**, 301 (2012).
- [59] C. Reichhardt, C. J. O. Reichhardt, and M. V. Milosevic, Statics and dynamics of skyrmions interacting with disorder and nanostructures, *Rev. Mod. Phys.* **94**, 035005 (2022).